Dicer-dependent and -independent Argonaute2 Protein Interaction Networks in Mammalian Cells*[S]

Anne Frohn‡§, H. Christian Eberl¶, Julia Stöhr§, Elke Glasmacher‖‡‡, Sabine Rüdel§, Vigo Heissmeyer‖, Matthias Mann¶, and Gunter Meister‡§**

Argonaute (Ago) proteins interact with small regulatory RNAs such as microRNAs (miRNAs) and facilitate gene-silencing processes. miRNAs guide Ago proteins to specific mRNAs leading to translational silencing or mRNA decay. In order to understand the mechanistic details of miRNA function, it is important to characterize Ago protein interactors. Although several proteomic studies have been performed, it is not clear how the Ago interactome changes on miRNA or mRNA binding. Here, we report the analysis of Ago protein interactions in miRNA-containing and miRNA-depleted cells. Using stable isotope labeling in cell culture in conjunction with Dicer knock out mouse embryonic fibroblasts, we identify proteins that interact with Ago2 in the presence or the absence of Dicer. In contrast to our current view, we find that Ago-mRNA interactions can also take place in the absence of miRNAs. Our proteomics approach provides a rich resource for further functional studies on the cellular roles of Ago proteins. ***Molecular & Cellular Proteomics 11: 10.1074/mcp.M112.017756, 1442–1456, 2012.***

Argonaute proteins are a highly conserved protein family found in all kingdoms of life (1, 2). They directly interact with small RNAs and can be classified according to the small RNA class they bind. The Argonaute (Ago)[1] subfamily is ubiquitously expressed and interacts with short interfering RNAs or miRNAs to mediate post-transcriptional gene silencing processes (3, 4). Expression of the Piwi subfamily of Argonaute proteins seems to be restricted to the germline, where they bind to Piwi interacting RNAs and inhibit the expression of mobile genetic elements (5).

Argonaute proteins contain Piwi-Argonaute-Zwille, MID, and PIWI domains. Structural analysis revealed that the Piwi-Argonaute-Zwille domain binds the 3′ end, whereas the MID domain specifically anchors the 5′ end of the bound small RNA (6). The PIWI domain is structurally similar to RNase H and indeed some Argonaute proteins possess endoribonuclease activity. Such proteins are referred to as "slicers" (7, 8).

MiRNAs, the main binding partners of Ago subfamily members in mammals, are transcribed by RNA polymerase II as capped and polyadenylated primary miRNA transcripts (4, 5, 9). In the nucleus, the microprocessor containing the RNase III enzyme Drosha processes primary miRNA transcripts to stem-loop structured precursors, which are exported to the cytoplasm. Here, the RNase III Dicer cleaves an approx. Twenty to twenty-three nucleotide (nt) long double stranded intermediate out of the stem of the pre-miRNA. The miRNA duplex is subsequently unwound and one strand gives rise to the mature miRNA whereas the other strand, referred to as miRNA*, is removed by cellular degradation systems. In rare cases, both strands can be selected and function as mature miRNAs (*e.g.* miR-9 and miR-9*). The mature miRNA binds to Ago proteins and together with other proteins, a miRNA-protein complex, referred to as miRNP, is formed (4, 9).

MiRNAs guide miRNPs to partially complementary sequences often located on the 3′ untranslated region (UTR) of target mRNAs (10, 11). On the target mRNA, a member of the GW protein family (termed TNRC6A-C in mammals) interacts with the Ago protein and induces deadenylation of the target mRNA by recruiting cellular deadenylases. mRNAs with shortened poly(A) tails are either translationally silent or decapped and finally degraded by cellular mRNA decay systems (12).

MiRNA-guided gene silencing is important for almost all cellular processes. Therefore, miRNA function is heavily regulated at many different steps. First, regulation occurs on the various steps of miRNA biogenesis including transcription and processing by Drosha and Dicer (13). Second, Ago protein

From the ‡Laboratory of RNA Biology, Max-Planck-Institute of Biochemistry, Am Klopferspitz 18, 82152 Martinsried; §Biochemistry Center Regensburg (BZR), Laboratory for RNA Biology, University of Regensburg, Universitätsstrasse 31, 93053 Regensburg; ¶Department of Proteomics and Signal Transduction, Max-Planck-Institute of Biochemistry, Am Klopferspitz 18, 82152 Martinsried; ‖Helmholtz Zentrum München, German Research Center for Environmental Health, Marchioninistr. 25, 81377 Munich, Germany

Received February 6, 2012, and in revised form, August 6, 2012
Published, MCP Papers in Press, August 23, 2012, DOI 10.1074/mcp.M112.017756

[1] The abbreviations used are: Ago, Argonaute; miRNAs, microRNAs; SILAC, stable isotope labeling in cell culture; MEFs, mouse embryonic fibroblasts; nt, nucleotide; Dnd 1, Dead end 1; mRNP, mRNA-protein complex; AP-MS, affinity purification combined with mass spectrometric analysis; wt, wild type; F/H, FLAG/HA; RISC, RNA induced silencing complex; ES, embryonic stem; EDC, 1-ethyl-3-(3-dimethylaminopropyl)carbodiimide; FDR, false discovery rates.

levels as well as their activities can be regulated by phosphorylation, hydroxylation, or ubiquitinylation (14–16). Third, Ago proteins are embedded into large protein-RNA structures containing miRNAs as well as translationally repressed mRNAs (17–19). It is becoming more and more apparent that proteins within such RNA-protein complexes (RNPs) can influence miRNA-guided gene silencing activity. For example, RNA binding proteins such as Dead end 1 (Dnd 1) can regulate accessibility of miRNA target sites (20). Another example is the ARE binding protein HuR, which antagonizes miRNA function by interfering with miRNA-target site interactions (21). Furthermore, the RNA binding protein hnRNP-E2 can function as decoy for a specific mature miRNA (22). These examples highlight the importance of the protein composition of an mRNA-protein complex (mRNP) for miRNA-guided gene silencing.

A common approach to analyze protein complex composition is the combination of affinity purification with mass spectrometric analysis (AP-MS) (23). However, despite great advances in this technology, it can have potential limitations especially when used in a nonquantitative format. Indeed, due to improvements in preparation methods and instrument sensitivity the potential to identify false positive as interaction partners has increased. Consequently, samples need to be purified to a high degree, for example by double affinity purification. Such stringent purification approaches require a high amount of sample and risk losing relevant but substochiometric and weak interactions. Quantitative proteomic approaches present an elegant solution to these problems (24, 25). They directly distinguish between background binders and true interaction partners by quantification between sample and control. Thus, they facilitate high confidence identification of interaction partners from low stringency and single step purifications (26). SILAC is a widespread metabolic labeling technique used in quantitative proteomics (27). SILAC-based proteomics can be applied to compare different states of protein complexes, for example upon stimulation (24, 28) or between protein isoforms (29). The technique is also suitable for monitoring dynamic changes (30) and has already been used to identify miRNA targets (31–33).

Several semiquantitative proteomic studies (17, 18, 34) contributed to the present picture of the human Ago interactome. These studies focused on the identification of Ago interaction partners under normal cellular conditions and generally did not attempt to further classify or validate these interactions. To study miRNA functions, Dicer-depleted embryonic stem cells have been established (35–37). In these cells, canonical mature miRNAs are absent (38) leading to effects on differentiation into distinct cell lineages upon stimulation (35, 36). The absence of Dicer can also lead to changes in Ago protein localization (39).

The availability of Dicer-deficient cell lines that lack mature miRNAs opens the unique possibility to study and compare the interactome of miRNA-loaded (Dicer positive cells) and miRNA-unloaded (Dicer-deficient cells) Ago protein complexes in mammalian cells. Here, we present a SILAC-based quantitative proteomic analysis of Ago2-containing ribonucleoprotein complexes in the presence and absence of Dicer and mature miRNAs. For this purpose, we established Dicer wild type (wt) and Dicer-depleted MEFs that stably express FLAG/HA (F/H)-tagged Ago2. We analyzed the miRNA/Dicer requirements of the interactors and identified new interaction partners that specifically associate with Ago2 in the absence of Dicer and miRNAs. Unexpectedly, we find that Ago2 still associates with mRNAs in the absence of miRNAs. Based on our proteomics data, we present an in depth and specific RNA-dependent and -independent Ago2 interaction network.

EXPERIMENTAL PROCEDURES

Lysate Preparation and Immunoprecipitation—SILAC labeled cells were lysed separately in Lysis Buffer (150 mM KCl, 25 mM Tris-HCl, pH 7.5, 2 mM EDTA, 1 mM NaF, 5% glycerol, 0,5% Nonidet P-40, 0,5 mM dithiothreitol, 1× Complete Protease Inhibitor mixture (Roche). For immunoprecipitation 3–4 mg total lysate protein were incubated with 50 μl M2 FLAG agarose beads (Sigma) for 4 h at 4 °C with rotation. For RNA dependence samples 100 μg/ml RNase A was added to the lysate for the last 20 min of the incubation. Beads were washed three times with IP Wash Buffer (300 mM KCl, 50 mM Tris-HCl pH 7.5, 5 mM $MgCl_2$, 0.1% Nonidet P-40, 5% glycerol) and twice with Elution Buffer (150 mM NaCl, 25 mM Tris-HCl pH 7.5, 5 mM $MgCl_2$, 5% glycerol). Corresponding beads for the SILAC experiments were combined directly after washing and bound proteins were eluted with 500 μg/ml 3x FLAG peptide (N-MDYKDHDGDYKDHDIDYKDDDDK-C) in Elution Buffer for 90 min at 4 °C with 800 rpm.

Protein Digestion—Eluates were separated by one dimensional gel electrophoresis on 4–12% NuPAGE gels (Invitrogen, Carlsbad, CA) and visualized by staining with the NOVEX Colloidal Blue Stain Kit (Invitrogen). Lanes were cut into 8 slices and proteins were in-gel digested with trypsin (Promega, Madison, WI) (40) using iodacetamide as alkylation reagent. Peptides were concentrated and desalted using C_{18} StageTips (41, 42).

LC-MS/MS Analysis—Peptides were separated on line to the mass spectrometer by using an easy nano-LC system (Proxeon Biosystems, Dreieich, Germany). Four microliter samples were loaded with a constant flow of 700 nl/min onto a 15-cm fused silica emitter with an inner diameter of 75 μm (Proxeon Biosystems) packed in house with RP ReproSil-Pur C18-AQ 3 μm resin (Dr. Maisch). Peptides were eluted with a segmented gradient of 5–60% solvent B over 105 min with a constant flow of 250 nl/min. The nano-LC system was coupled to a mass spectrometer (LTQ-Orbitrap; Thermo Fisher Scientific) via a nanoscale LC interface (Proxeon Biosystems). The spray voltage was set between 2.0 and 2.2 kV, and the temperature of the heated capillary was set to 200 °C.

Survey full-scan MS spectra (m/z = 300–2000) were acquired in the Orbitrap with a resolution of 60,000 at the theoretical m/z = 400 after accumulation of 1,000,000 ions in the Orbitrap. The five most intense ions from the preview survey scan delivered by the Orbitrap were sequenced by collision induced dissociation (collision energy 35%) in the LTQ after accumulation of 5000 ions concurrently to full scan acquisition in the Orbitrap. Maximal filling times were 1000 ms for the full scans and 150 ms for the MS/MS. Precursor ion charge state screening was enabled, and all unassigned charge states as well as singly charged peptides were rejected. The dynamic exclusion list was restricted to a maximum of 500 entries with a maximum retention period of 90 s and a relative mass window of 10 ppm. Orbitrap measurements were performed with the lock mass option enabled for

survey scans to improve mass accuracy (polydimethylcyclosiloxane (PCM) ions at *m/z* 445.120025) (43).

The raw files were processed using the MaxQuant computational proteomics platform (44) version 1.1.1.27. The fragmentation spectra were searched against the IPI mouse database (version 3.68, 56,729 entries) supplemented with frequently observed contaminants, using the Andromeda search engine (45) with the initial precursor and fragment mass tolerances set to 7 ppm and 0.5Da, respectively, and with up to two missed cleavages allowed. Trypsin allowing for cleavage N-terminal to proline was chosen as enzyme specificity. Carbamidomethylated cysteins were set as fixed, oxidation of methionine, and N-terminal acetylation as variable modifications. Maximum false discovery rates (FDRs)—calculated by employing a reverse database strategy—were set to 0.01 both on peptide and protein levels and thus not dependent on the peptide score. Minimum required peptide length was six amino acids. Corresponding forward and reverse experiments were analyzed together and specified as "forward" and "reverse" in the experimental design.

Raw MS data, unfiltered protein groups tables and peptides tables can be downloaded from https://proteomecommons.org/tranche using the following HASH key:

a6LrT+dbaF4jmWZcpYPJuvlzNTFmI0VhkHfqhh4SwQ8l68MSFv5dnfBw35h8RNo99yQZUIAhTvWHpL+xXo7dW25eigAAAAAAAABXfA==.

All further analysis was done in a script-based manner employing R (http://www.r-project.org). Protein groups were further filtered requiring at least two unique peptides per protein identification, and 2 ratio counts (quantification events) in the forward as well as in the reverse experiment. For all analysis log2 transformed normalized ratios (as computed by MaxQuant) were used.

Median plus 1.2 standard deviations and median minus 1.2 standard deviations was used as significance threshold in the forward and reverse experiment, respectively. Proteins were defined as interactors if they passed the threshold either in the wt *versus* control, or the knockout *versus* control experiment in the forward and reverse experiment. For all further analysis, only proteins passing these criteria were considered. For hierarchical clustering only proteins that showed a ratio in four out of six experiments (wt *versus* control, ko *versus* control, wt *versus* ko; each forward and reverse) were considered.

The separate experiments were combined using the Uniprot identifier, and proteins were clustered employing an Euclidian distance matrix.

RESULTS

Generation of MEFs Stably Expressing Tagged Ago2—To identify Dicer-dependent and -independent Ago2 interactors, we established Dicer-deficient or Dicer wt MEF cell lines that stably express FH-tagged Ago2 (Fig. 1). We confirmed the stability of the Dicer knock out during culturing by PCR (Fig. 1*A*) and tested FH-Ago2 expression levels by Western blotting using antibodies against the HA-tag (Fig. 1*B*). As expected and also observed for endogenous Ago proteins (data not shown), FH-Ago2 levels are slightly lower in the Dicer-deficient cells compared with Dicer wt cells. This is probably due to active destabilization of unloaded Ago proteins. The GFP-only expressing cell lines serve as controls for all experiments. To minimize background binding during our biochemical Ago2 complex purification, we asked whether FH-Ago2 can be eluted with the FLAG-peptide (Fig. 1*C*). Indeed, an excess of FLAG-peptide efficiently removed bound FH-Ago2 from the anti-FLAG antibody matrix. As a further quality control, we analyzed miRNA expression in Dicer-deficient MEFs that express FH-Ago2 (Fig. 1*D*). Northern blotting against miR-19b showed that miRNAs were neither present in the lysates of Dicer-deficient MEFs nor in anti-FLAG immunoprecipitates from these cells. Therefore, the cell lines are suitable for the analysis of miRNA-dependent and -independent Ago2 interaction partners.

To further increase the robustness and information content of our quantitative mass spectrometry data, we performed forward and reverse (label swapping) experiments. For the forward experiment, we labeled the FH-Ago2-expressing cell line with heavy amino acids and the corresponding GFP-expressing cell line with light amino acids (Fig. 1*E*, *left* panel). For the reverse experiment, the labels of the cell lines were swapped (*right* panel). To prevent potential heavy to light exchange of specific transiently interacting partners during the purification procedure (46, 47), the FH-Ago2 complexes were immunoprecipitated with the FLAG antibody from total lysates for each SILAC state separately and combined during FLAG peptide elution. Eluates were separated by SDS-PAGE and cut into eight slices, proteins were in-gel digested and peptides were analyzed by high resolution LC-MS/MS on an LTQ Orbitrap instrument.

Specific interactors by definition show a high ratio in forward and a low ratio in reverse experiments, whereas unspecific background binders show a ratio close to 1 in both experiments. For data visualization, we plot the logarithmized normalized ratios of the forward and reverse experiments against each other. Every dot represents an identified and quantified protein. Each of the datasets contained on average 1214 identified proteins and 672 of these fulfilled our strict criteria for quantification (see Experimental procedures). Background binders constitute the vast majority of quantified proteins show no ratio change between SILAC pairs and are therefore clustered around zero (Fig. 1*F*, *gray* circle). Specific Ago2 interactors show high ratios in the forward and low ratios in the reverse experiment and are outliers from the background distribution in the lower right quadrant (*green* circle).

Identification of Dicer-independent Ago2 Interactors—To compare miRNA-free (unloaded) and miRNA-containing (loaded) Ago2 complex compositions, we isolated FH-Ago2 from Dicer wt and Dicer-depleted cell lines. GFP-transfected cells were used to identify unspecific binders (Fig. 2). Proteins interacting with Ago2 independently of miRNAs show significant ratios above the cut-off both in Dicer +/+ and Dicer −/− cell lines when measured against the GFP control (Fig. 2*A*, *left* and *middle* panel; specific binders appear in the lower right quadrant). To directly quantify the interaction as a function of the presence or absence of Dicer and miRNAs, we additionally precipitated FH-Ago2 from Dicer +/+ MEFs (heavy label) and Dicer −/− MEFs (light label). Labels were swapped for the reverse experiment. In this experiment, proteins binding independently of miRNAs appear together with the background binders clustering around zero (*right* panel).

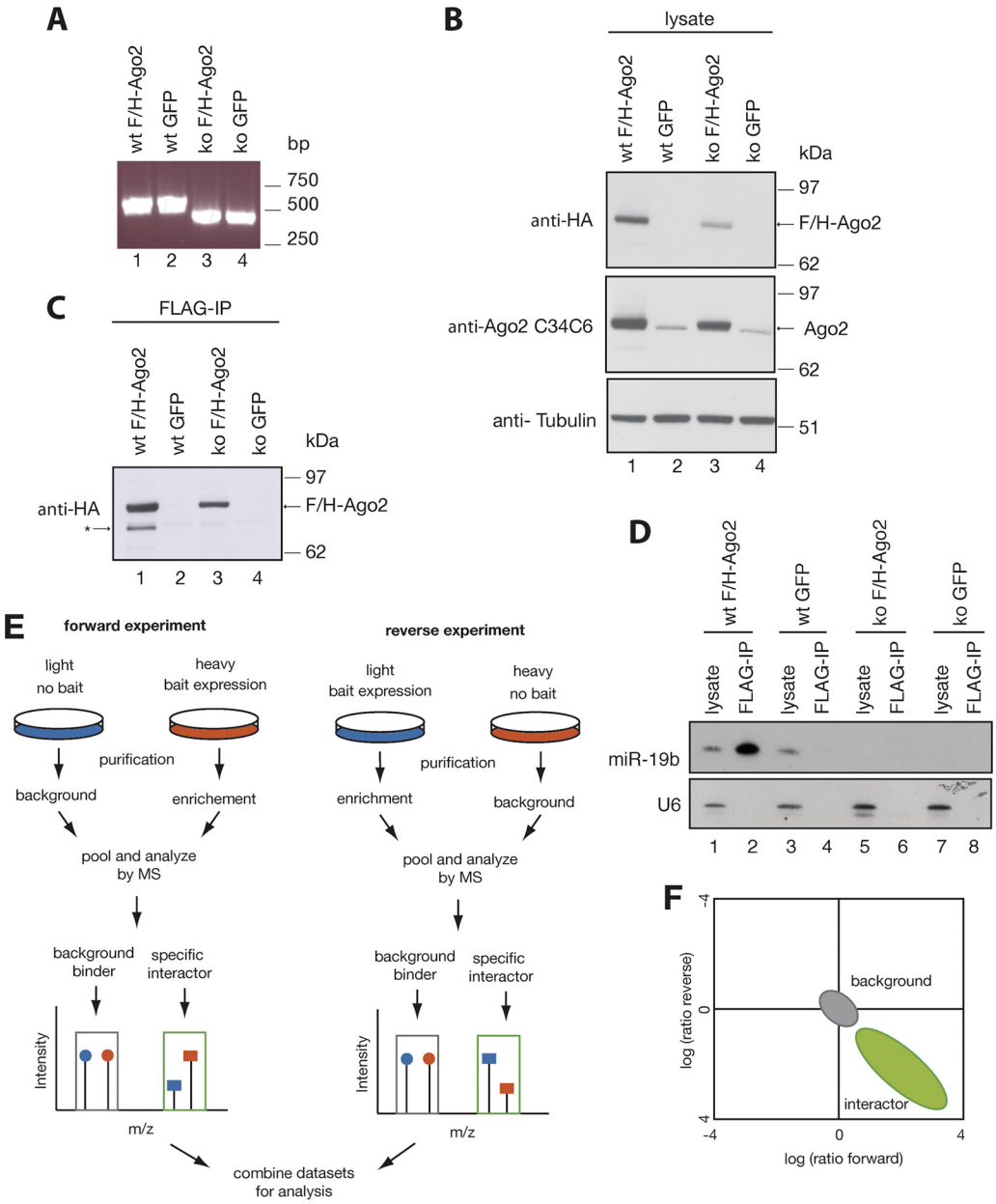

FIG. 1. **Characterization of the F/H-Ago2 expressing MEFs.** *A*, Wild type (wt) and Dicer-depleted (ko) MEFs were transduced with an adenovirus carrying F/H-Ago2 and GFP. Genomic DNA was isolated from cells 3 weeks after transduction and amplified by PCR with primers flanking the deleted region in the Dicer gene. PCR products were separated on an agarose gel and visualized by Ethidiumbromide staining. *B*, Expression of F/H-Ago2 was analyzed by Western blotting. Total cell lysates were separated by SDS-PAGE, blotted and probed with anti-HA (*upper* panel), anti-Ago2 (*middle* panel) or anti-tubulin antibodies (*lower* panel). *C*, Proteins were immunoprecipitated from total lysate with anti-FLAG agarose beads and bound proteins were eluted from the antibody with 3xFLAG peptide. Eluted proteins were analyzed by Western blotting with anti-HA antibodies. The asterisk indicates a degradation product. *D*, RNA was isolated from lysate or immunoprecipitated F/H-Ago2, separated by 12% denaturing PAGE, blotted and probed for miR-19b (*upper* panel) or U6 (*lower* panel). *E*, Schematic representation of SILAC-based interaction proteomics. For the forward experiment (*left* panel), the F/H-Ago2-expressing cell line (bait expression) was labeled with heavy amino acids (*red*) and the corresponding GFP-expressing cell line (no bait) was labeled with light amino acids (*blue*). For the reverse experiment (*right* panel), the SILAC label was swapped. *F*, Forward and reverse data sets are combined for analysis. For data visualization, the logarithmized normalized ratios of the forward and reverse experiments are plotted against each other. Background binders are clustered around zero, as highlighted by the *gray* circle. Specific interactors can be found in the lower right quadrant as indicated by the *green* circle.

Among the Dicer-independent Ago2 binders (Table I; see supplemental Table S1 for the complete mass spec data set), we found a number of proteins that have been implicated in Ago2 function before, indicating high specificity in our analyses. For example, Hsp90 is involved in loading small RNAs into RISC (48, 49) and it regulates Ago2 localization (50). The

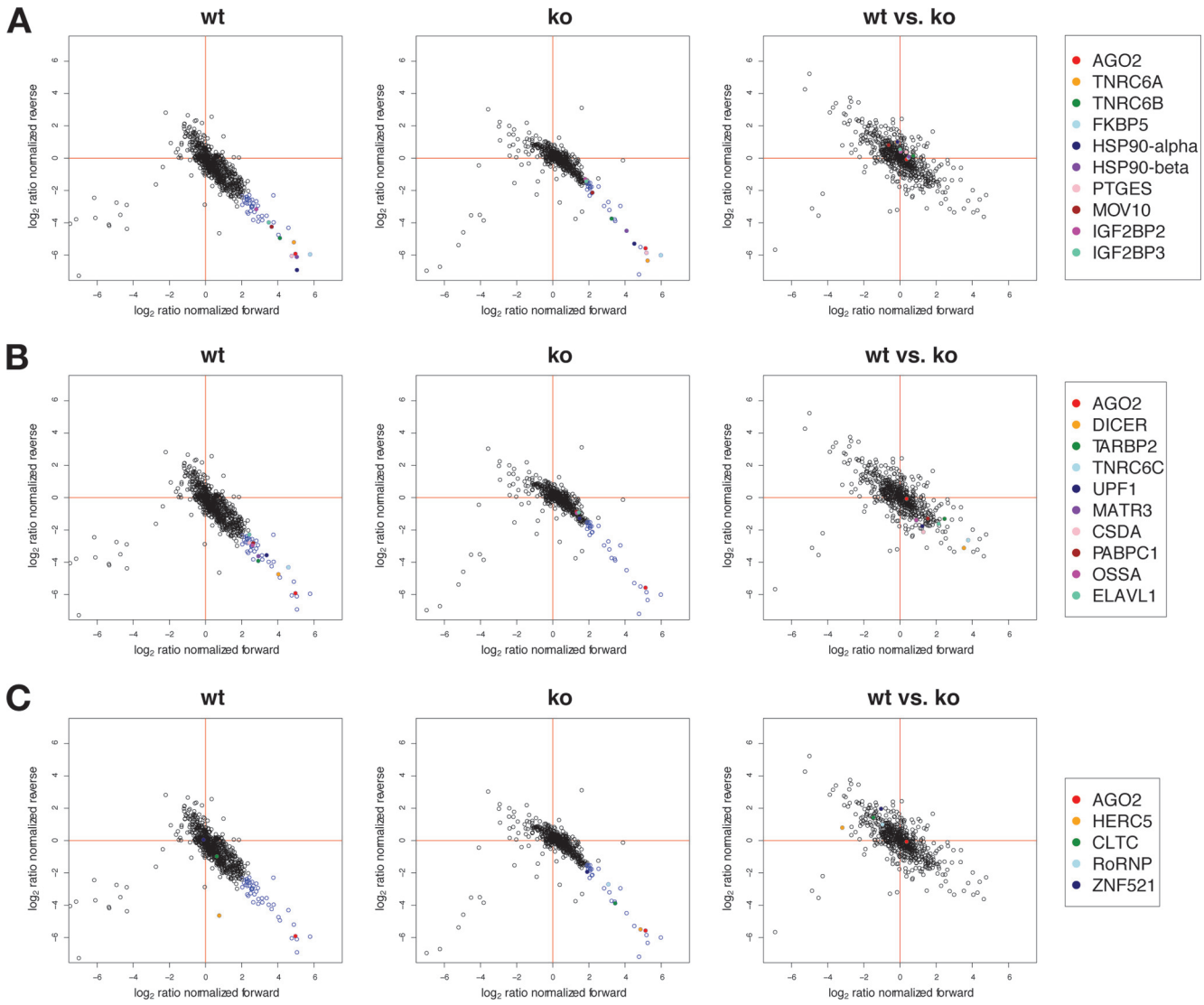

FIG. 2. **Identification of proteins associating with Ago2 independently of Dicer.** Logarithmized normalized ratios of forward and reverse experiments for F/H-Ago2 immunoprecipitations from Dicer-expressing MEFs (*left* panel) and the Dicer-depleted MEFs (*middle* panel) *versus* their corresponding control cell lines are plotted as described in Fig. 1*F*. To compare miRNA-free and miRNA-containing complexes, F/H-Ago2 was immunoprecipitated from SILAC-labeled Dicer wt and Dicer-depleted cell lines with the FLAG-antibody and further analyzed as described in Figs. 1*E* and 1*F* (*right* panel). All outliers are shown as *blue* circles, while black circles indicate background binders. Selected Ago2 binding partners are highlighted with different colors. *A*, In this experimental setup, proteins associated with Ago2 independently of miRNA presence or absence cluster around zero in a ratio plot (*right* panel). *B*, Same plots as in (*A*). Selected proteins binding to Ago2 preferentially in the presence of Dicer and miRNAs are indicated in color. *C*, Proteins interacting with Ago2 preferentially in the absence of Dicer and miRNA are indicated in colors in ratio plots of immunoprecipitation experiments from Dicer expressing MEFs (*left*), Dicer-depleted MEFs (*middle*) and Dicer expressing *versus* Dicer-depleted MEFs (*right*) that were generated as described in Fig. 2*A*.

co-chaperones FKBP5 and PTGES have not been described in Ago2 complexes before and but our results suggest that they may function in a similar manner. Another example is the putative DExD box helicase MOV10, which has been identified as RISC component before (17, 18, 34). Other proteins in this group are the mRNA binding proteins IGF2BP1–3, PUM2, DHX30, HNRNPL, a highly specific set of ribosomal proteins (RPS 19, 18, 14, 5, and 3a) and the ARE binding protein DHX36/RHAU. We also find proteins involved in mRNA decay such as the decapping enhancer EDC4, Upf1 and DDX6/Rck (51–53). As mentioned above, GW proteins directly interact with Ago proteins via a specific Ago-interaction domain (12) and consistently, we find TNRC6A and TNRC6B as Dicer-independent Ago2 binders. Finally, the novel Ago2 interacting protein STRAP/Unrip (54) found here has been shown to interact with poly-A binding proteins and are involved translational repression in *Drosophila* (55). We speculate that this protein is involved in miRNA-guided gene silencing as well.

Identification of Dicer-dependent Ago2 Interactors—We next analyzed proteins that bind to Ago2 preferentially in the

TABLE I
Dicer dependent and independent Ago2 interactors

Protein names	Gene names	Uniprot	Keywords	wt		knockout		wt *vs* knockout	
				Ratio normalized Forward	Ratio normalized Reverse	Ratio normalized Forward	Ratio normalized Reverse	Ratio normalized Forward	Ratio normalized Reverse
Bait protein: Ago2									
Protein argonaute-2	Eif2c2;Ago2	A1A563	small RNA mediated gene silencing	31.401	0.017	35.089	0.021	1.2876	0.952
Proteins binding independently of the presence or absence of miRNAs/Dicer									
Peptidyl-prolyl cis-trans isomerase FKBP5	Fkbp5	Q64378	heteromultimeric cytoplasmic complex with HSP90 and HSP70	55.043	0.016	63.056	0.016	1.377	1.017
Heat shock protein HSP 90-alpha	Hsp90 alpha	P07901	molecular chaperone ATPase activity	33.307	0.008	22.783	0.026	0.90288	2.010
Heat shock protein 84b	Hsp90 beta	Q71LX8	molecular chaperone ATPase activity	33.102	0.015	16.950	0.044	1.4013	1.066
Trinucleotide repeat-containing gene 6A protein	Tnrc6a	Q3UHK8	small RNA mediated gene silencing	29.605	0.027	37.910	0.012	0.87774	1.995
Cytosolic prostaglandin E2 synthase	Ptges3	Q9R0Q7	molecular chaperone	27.236	0.015	36.365	0.017	1.27	1.301
Trinucleotide repeat-containing gene 6B protein	Tnrc6b	Q8BKI2-1	small RNA mediated gene silencing	17.280	0.032	9.537	0.075	1.6645	1.106
Insulin-like growth factor 2 mRNA-binding protein 1	Igf2bp1	O88477	RNA binding, mRNA translation and stability	13.611	0.064	2.622	0.537	0.57078	2.068
Putative helicase MOV-10	Mov10	Q3TFC0	small RNA mediated gene silencing	12.604	0.053	4.575	0.229	0.6453	1.757
Insulin-like growth factor 2 mRNA-binding protein 3	Igf2bp3	Q9CPN8	RNA binding, mRNA translation and stability	11.289	0.064	3.601	0.372	1.0019	1.452
Pumilio homolog 2	Pum2	Q80U58-1	mRNA translation and stability, mRNA 3′UTR binding	8.727	0.084	no value	no value	1.9104	0.635
Insulin-like growth factor 2 mRNA-binding protein 2	Igf2bp2	Q5SF07-1	mRNA translation, mRNA 5′UTR binding	6.983	0.112	3.477	0.406	1.0228	1.330
Probable ATP-dependent RNA helicase DHX36	Ddx36	Q8VHK9	mRNA degradation, mRNA deadenylation	6.003	0.125	2.961	0.379	1.1648	0.585
Putative ATP-dependent RNA helicase DHX30	Dhx30	Q99PU8-3	RNA binding, ATP dependent helicase	5.459	0.166	2.308	0.483	1.6228	0.454
YTH domain family 2	Ythdf2	Q3TWU3	unknown function	4.820	0.175	3.732	0.350	no value	no value
40S ribosomal protein S14	Rps14	P62264	ribosomal protein	4.387	0.280	4.217	0.298	1.4352	0.685
Heterogeneous nuclear ribonucleoprotein L	Hnrnpl	Q8R081	pre-mRNA binding	4.080	0.198	2.338	0.780	no value	no value
Ribosomal protein S5;Ribosomal protein S5	Rps5	Q91V55	ribosomal protein	3.951	0.299	4.169	0.273	1.3374	0.740
40S ribosomal protein S19	Rps19	Q5M9P3	ribosomal protein	3.558	0.369	4.152	0.287	1.3051	0.827
40S ribosomal protein S18	Rps18	P62270	ribosomal protein	3.534	0.379	4.171	0.347	1.2577	0.765
40S ribosomal protein S3a	Rps3a	P97351	ribosomal protein	3.337	0.362	4.435	0.294	1.37	0.776
Histone H1.4	H1f4	P43274	chromatin compaction	3.063	0.229	3.692	0.337	1.5909	0.665
Heterochromatin protein 1-binding protein 3	Hp1bp3	Q3TEA8-1	unknown function	2.229	0.248	5.788	0.297	0.81516	1.439
Probable ATP-dependent RNA helicase DDX6	Ddx6	P54823	mRNA degradation mRNA decapping	no value	no value	7.152	0.129	1.8026	1.118
Enhancer of mRNA-decapping protein 4	Edc4	Q3UJB9-1	mRNA decapping	no value	no value	8.772	0.108	1.0429	0.785

TABLE I—*continued*

Protein names	Gene names	Uniprot	Keywords	wt		knockout		wt *vs* knockout	
				Ratio normalized Forward	Ratio normalized Reverse	Ratio normalized Forward	Ratio normalized Reverse	Ratio normalized Forward	Ratio normalized Reverse
Proteins binding preferentially in the presence of miRNAs/Dicer									
Trinucleotide repeat-containing gene 6C protein	Tnrc6c	Q3UHC0	small RNA-mediated gene silencing	23.986	0.050	no value	no value	13.655	0.161
Endoribonuclease Dicer	Dicer	Q8R418	small RNA-mediated gene silencing	16.371	0.037	no value	no value	11.599	0.115
Regulator of nonsense transcripts 1	Rent1;Upf1	Q9EPU0-1	nonsense mediated mRNA decay	10.406	0.085	2.786	0.411	2.3498	0.294
Matrin-3	Matr3	Q8K310	RNA binding nuclear matrix	7.601	0.081	no value	no value	1.8666	0.378
RISC-loading complex subunit TARBP2	Tarbp2	Q99M41	small RNA-mediated gene silencing	7.550	0.066	no value	no value	5.5222	0.403
Nuclease-sensitive element-binding protein 1	Ybx1	P62960	transcription pre-mRNA splicing mRNA processing	7.006	0.158	3.917	0.348	4.4745	0.300
Polyadenylate-binding protein 1	Pabp1	P29341	poly(A) tail of mRNA binding	6.248	0.142	2.471	0.549	2.9082	0.408
Constitutive coactivator of PPAR-gamma-like protein 1	FAM120A	Q6A0A9	RNA binding oxidative stress	6.071	0.129	2.512	0.516	1.861	0.385
ELAV-like protein 1	Elavl1	P70372	AU-rich element binding	5.352	0.204	2.716	0.530	4.4003	0.325
Cold shock domain-containing protein A	Csda	Q9JKB3-1	mRNA binding translational repression transcription	5.349	0.144	no value	no value	2.4444	0.229
Poly(A) binding protein, cytoplasmic 4	Pabpc4	Q99LF8	RNA binding	5.161	0.178	2.166	0.651	3.4872	0.311
Heterogeneous nuclear ribonucleoproteins C1/C2	Hnrnpc	Q3U6P5	pre-mRNA binding mRNA binding	5.136	0.093	1.691	0.919	2.0791	0.446
ATP-dependent RNA helicase A	Ddx9	O70133-2	transcription RNA binding, helicase	4.962	0.099	1.676	0.764	2.5389	0.685
La-related protein 1	Larp1	Q6ZQ58-1	RNA binding	4.932	0.169	1.718	0.581	2.5641	0.464
Fragile X mental retardation syndrome-related protein 1	Fxr1	Q61584-1	RNA binding	4.897	0.191	2.945	0.386	2.713	0.469
Fragile X mental retardation syndrome-related protein 2	Fxr2	Q3TA75	RNA binding	4.806	0.190	2.855	0.360	no value	no value
Heterogeneous nuclear ribonucleoprotein U-like protein 1	Hnrnpul1	Q8VDM6-1	transcription mRNA processing and transport	4.388	0.161	no value	no value	2.0873	0.438
Proteins binding preferentially in the absence of miRNAs/Dicer									
Putative uncharacterized protein	Herc5	Q3UEA7	E3 ubiquitin-protein ligase ISGylation	1.690	0.040	28.888	0.022	0.10923	1.732
Clathrin heavy chain 1	Cltc	Q5SXR6	vesicel coating	1.537	0.507	10.934	0.068	0.36005	2.680
Zinc finger protein 521	Zfp521	Q6KAS7-1	transcription factor	0.923	1.034	3.739	0.261	0.48416	3.891
Protein argonaute-3	Ago3	Q8CJF9	small RNA-mediated gene silencing	2.976	0.176	13.360	0.129	no value	no value
60 kDa SS-A/Ro ribonucleoprotein	Ssa2; RoRNP	O08848	RNA binding	no value	no value	8.421	0.1527	0.51235	1.990

presence of Dicer and miRNAs (Fig. 2*B*). Together with Dicer itself, this group of proteins is located in the lower right quadrant in the experiments using Dicer +/+ cells *versus* control (Fig. 2*B*, *left* panel) and in the Dicer +/+ *versus* Dicer −/− experiment (*right* panel). In the Dicer −/− *versus* control experiment, these proteins do not appear as specific binders (*middle* panel).

As expected, we find the Dicer cofactor TARBP2 (TRBP) (56, 57) in this group (Table I). Among the identified factors is the RNA helicase A/DHX9, which has been implicated in siRNA-loading (58). Proteins such as YBX1, Gemin4, Gemin5, HNRNPC, HNRNPUL1, the ARE binding protein ELAVL1/HuR, the poly-A binding proteins PABPC1 and 4, the mitochondrial protein Matrin3 and the Fragile X mental retardation protein paralog FXR2 have been found in Ago complex purifications before. In addition, we identified the PABPC1-binding protein LARP1 (59), the mRNA binding proteins FAM120A/Ossa and CSDA, which have not been implicated in Ago2 function before. In contrast to the GW protein family members TNRC6A and B, TNRC6C interacts with Ago2 only in the presence of Dicer, suggesting that it requires Ago2 to be loaded onto miRNA target mRNAs. Of note, it is also conceivable that proteins found in this group associate with Ago2 indirectly via interaction with Dicer.

Proteins that Interact with Ago2 Preferentially in the Absence of Dicer—Proteins that preferentially interact with unloaded Ago2 are found in the lower right quadrant of the plot generated from Dicer-deficient cells (Fig. 2*C*, *middle* panel).

In this group, we find the RNA binding protein RoRNP (60), the zinc finger protein ZNF521 (61) and the vesicle coat protein clathrin (CLTC) (Table I). Of note, Ago3 shows an increased association with Ago2 in the absence of Dicer and miRNAs. HERC5, a HECT-type E3 protein ligase that mediates conjugation of ISG15 to target proteins in human (62) is also in this group, raising the possibility that it post-translationally modifies unloaded Ago2.

Ago2 Associates with mRNPs in the Absence of Dicer and Mature miRNAs—Because miRNAs guide Ago proteins to specific mRNAs for gene silencing, RNA-binding proteins are associated with Ago proteins and many of these interactions are bridged by mRNAs (17–19, 34). However, a requirement for miRNA for these interactions have generally not been investigated. To our surprise, we noticed that several mRNA binding proteins bind to Ago2 independently of Dicer and mature miRNAs. Some of these proteins associate with Ago2 in an RNA-dependent manner as has been reported for IGF2BP1 and three for example (17) suggesting that Ago2 may associate with mRNAs even in the absence of mature miRNAs. To test this hypothesis, we immunoprecipitated Ago2 complexes from the F/H-Ago2 expressing Dicer wt and Dicer-depleted MEFs and isolated the bound RNAs (Fig. 3*A*). GFP expressing cell lines or RNase treatment served as control. The isolated RNAs were analyzed on an agarose gel and Ago2 levels were controlled by Western blotting. A significant amount of longer RNA is bound to Ago2 in the Dicer-depleted cells supporting our hypothesis that Ago2 stably associates with mRNAs in the absence of miRNAs (Fig. 3*A*).

Because Ago2 may interact with mRNAs in the absence of miRNAs, it was not clear from our SILAC data which interactions were mediated by mRNAs. To analyze mRNA-bridged Ago2 interactions, we established RNase treatment conditions under which the mRNA is completely degraded but the miRNAs are not affected (supplemental Fig. S1). We performed a SILAC experiment in which Ago2-containing mRNPs were isolated and the immunoprecipitate from the light labeled cells was treated with RNase A whereas the immunoprecipitate from the heavy labeled cells was untreated. For reverse experiments, labels were swapped. We obtained 681 quantified proteins in the Dicer wt and 520 in the Dicer-depleted cell lines (supplemental Table S2). We exclusively considered the proteins that were identified as specific interactors in our previous experiment (Table I) and visualized their ratios in plots (Fig. 3*B*), a heat map (Fig. 3*C*) as well as a table (Table II). In the ratio plots, RNA-dependent interactors appear in the lower right quadrant and interactors that are not affected by RNase treatment appear together with the background binders in the center of the ratio plots. In the heat map, the red color indicates values above, blue below and gray around zero. Red-blue pairs for forward and reverse experiments are characteristic for an mRNA-dependent interactor.

As hypothesized, a high number of proteins associate with Ago2 in a RNA-dependent manner even in the absence of miRNAs (Table II). In this group, we find many RNA binding proteins including IGF2BP1–3, DHX36, DHX30, HNRNPL, and the ribosomal protein RPS14. Strikingly, genetic data in *C. elegans* demonstrated that PRS14 modulates mature let-7 function (63). The SILAC data therefore confirms that Ago proteins associate with mRNAs in the absence of mature miRNAs.

Additionally, we find RNA-dependent interactors that are only present when miRNAs are present (Table II). Among them are UPF1, FAM120A, YBX1, CSDA, ELAVL1/HuR, Matrin3, HNRNPC and LARP1. Interestingly, the poly-A binding proteins 1 and 4 also appear to require miRNAs for RNA-dependent Ago2 association.

A set of proteins associates with Ago2 in an mRNA-independent manner. This includes the TNRC6 proteins and Dicer. Other miRNA-independent protein-protein interactors of Ago2 are the HSP90 alpha and beta proteins with their cochaperones PTGES and FKBP5. Among the interactors preferentially binding in the absence of Dicer and miRNAs only Ago3, CLTC and ZNF521 were identified in the datasets and they show a direct binding behavior.

Taken together, our mass spectrometry approach revealed that Ago2 associates with larger RNA species even in the absence of small RNAs. Furthermore, several mRNA-binding proteins are specific to miRNA-free and miRNA-containing Ago2-mRNA complexes.

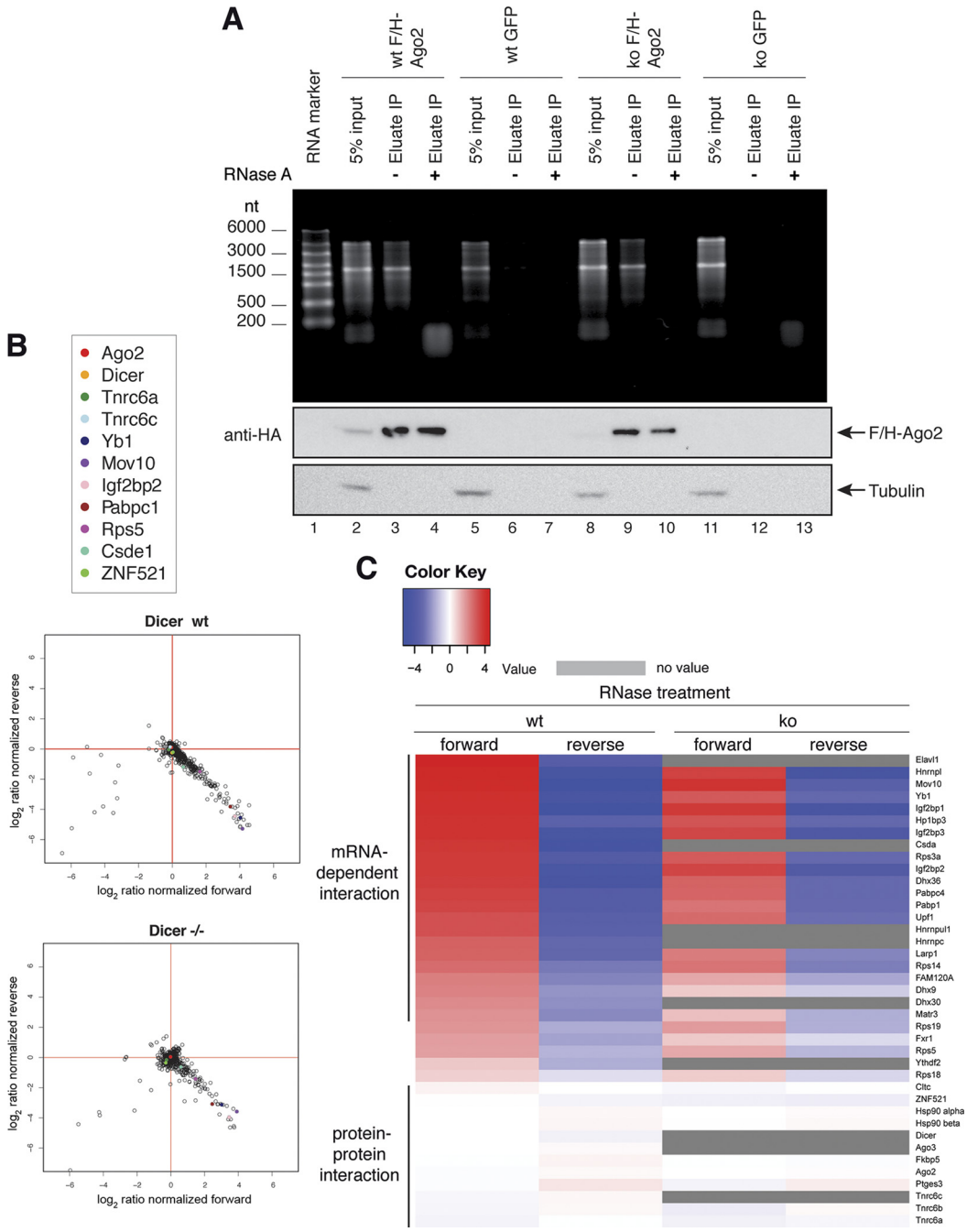

FIG. 3. **Dicer- and miRNA-independent mRNA binding of Ago2.** *A*, Ago2-containing RNPs were precipitated from whole cell lysate of Dicer wt (lanes 1–3) and Dicer-depleted (lanes 8–10) MEFs and treated with RNase A as indicated. GFP-only expressing cell lines were used as negative controls (lanes 5–7 and 11–13). RNA was isolated from immunoprecipitates or lysates were separated on an agarose gel and visualized by ethidiumbromide staining (*upper* panel). F/H-Ago2 was analyzed by Western blotting with anti-HA antibodies (*middle* panel). Tubulin was used as a loading control (*lower* panel). *B*, To analyze the mRNA requirements for Ago2 interactions, F/H-Ago2 was immunoprecipitated from total cell lysates from SILAC labeled, F/H-Ago2-expressing Dicer wild type (wt) MEFs. One sample was treated with RNase A and beads were combined for elution after washing. Eluates were analyzed by LC-MS/MS and the data is visualized in ratio plots as described in Fig. 1*F* (*upper* panel). The experiments were also carried out using the F/H-Ago2-expressing Dicer-depleted MEFs (lower panel). The mRNA-dependent Ago2 interactors are expected to show high H/L ratios in the forward and low ratios in the reverse experiment and appear in the lower right quadrant. Selected Ago2 interactors are indicated in color. *C*, The H/L ratios of Ago2 interactors (see Table I) in the RNase treatment experiment are displayed in form of a heat map. Red indicates values above, blue below and white around zero. Gray squares indicate that the protein was not identified in the experiment. Red-blue pairs for forward and reverse ratios are characteristic for an mRNA-dependent interactor. The color intensity indicates the strength of the mRNA dependence.

TABLE II
RNA dependent and independent Ago2 interactors

Protein names	Gene names	Uniprot	wt		knockout	
			Ratio normalized Forward	Ratio normalized Reverse	Ratio normalized Forward	Ratio normalized Reverse
Bait protein: Ago2						
Protein argonaute-2	Eif2c2;Ago2	A1A563	0.964	1.077	0.988	1.030
mRNA dependent interactions						
Proteins binding preferentially in the presence of mRNAs						
Proteins binding independently of the presence or absence of miRNAs/Dicer						
Heterogeneous nuclear ribonucleoprotein L	Hnrnpl	Q8R081	18.787	0.039	11.405	0.040
Putative helicase MOV-10	Mov10	Q3TFC0	17.880	0.026	15.032	0.084
Insulin-like growth factor 2 mRNA-binding protein 1	Igf2bp1	O88477	16.224	0.028	13.345	0.043
Heterochromatin protein 1-binding protein 3	Hp1bp3	Q3TEA8-1	15.491	0.091	8.570	0.114
Insulin-like growth factor 2 mRNA-binding protein 3	Igf2bp3	Q9CPN8	15.403	0.040	10.633	0.058
40S ribosomal protein S3a	Rps3a	P97351	13.257	0.067	7.823	0.118
Insulin-like growth factor 2 mRNA-binding protein 2	Igf2bp2	Q5SF07-1	13.066	0.046	10.980	0.064
Probable ATP-dependent RNA helicase DHX36	Dhx36	Q8VHK9	12.600	0.042	6.981	0.117
40S ribosomal protein S14	Rps14	P62264	6.142	0.161	5.439	0.170
Putative ATP-dependent RNA helicase DHX30	Dhx30	Q99PU8-3	4.105	0.219	no value	no value
Proteins binding preferentially in the presence of miRNAs/Dicer						
ELAV-like protein 1	Elavl1	P70372	23.522	0.075	no value	no value
Nuclease-sensitive element-binding protein 1	Ybx1	P62960	16.441	0.042	8.083	0.115
Cold shock domain-containing protein A	Csda	Q9JKB3-1	14.131	0.035	no value	no value
Poly(A) binding protein, cytoplasmic 4	Pabpc4	Q99LF8	11.727	0.071	6.775	0.117
Polyadenylate-binding protein 1	Pabpc1	P29341	10.879	0.071	5.477	0.118
Regulator of nonsense transcripts 1	Rent1;Upf1	Q9EPU0-1	9.236	0.081	6.314	0.133
Heterogeneous nuclear ribonucleoprotein U-like protein 1	Hnrnpul1	Q8VDM6-1	9.222	0.088	no value	no value
Heterogeneous nuclear ribonucleoproteins C1/C2	Hnrnpc;Hnrpc	Q3U6P5	7.047	0.112	no value	no value
La-related protein 1	Larp1	Q6ZQ58-1	6.910	0.107	4.889	0.189
Protein FAM120A	FAM120A	Q6A0A9	4.762	0.186	2.808	0.299
ATP-dependent RNA helicase A	Dhx9	O70133-2	4.561	0.233	1.856	0.498
Matrin-3	Matr3	Q8K310	3.789	0.201	2.140	0.331
Proteins showing a weak preference for binding in the presence of mRNAs						
Proteins binding preferentially in the presence of miRNAs/Dicer						
Fragile X mental retardation syndrome-related protein 1	Fxr1	Q61584-1	3.208	0.276	1.885	0.601
Proteins binding independently of the presence or absence of miRNAs/Dicer						
40S ribosomal protein S19	Rps19	Q5M9P3	3.604	0.319	3.291	0.332
40S ribosomal protein S5	Rps5	Q91V55	3.115	0.356	2.764	0.374
YTH domain family 2	Ythdf2	Q3TWU3	1.915	0.329	no value	no value
40S ribosomal protein S18	Rps18	P62270	1.755	0.646	1.804	0.581
mRNA independent, direct protein-protein interactions						
Proteins binding preferentially in the presence of miRNAs/Dicer						
Endoribonuclease Dicer	Dicer	Q8R418	0.992	0.843	no value	no value
Trinucleotide repeat-containing gene 6C protein	Tnrc6c	Q3UHC0	0.916	1.101	no value	no value
Proteins binding independently of the presence or absence of miRNAs/Dicer						
Heat shock protein HSP 90-alpha	Hsp90aa1	P07901	1.005	1.096	1.007	1.055
Heat shock protein 84b	Hsp90ab1	Q71LX8	1.003	1.118	1.018	1.084
Peptidyl-prolyl cis-trans isomerase FKBP5	Fkbp5	Q64378	0.973	1.147	0.980	0.968
Prostaglandin E synthase 3	Ptges3	Q9R0Q7	0.960	1.345	0.861	1.242
Trinucleotide repeat-containing gene 6B protein	Tnrc6b	Q8BKI2-1	0.894	1.080	0.784	1.073
Trinucleotide repeat-containing gene 6A protein	Tnrc6a	Q3UHK8	0.865	0.975	0.836	0.896
Proteins binding preferentially in the absence of miRNAs/Dicer						
Clathrin heavy chain 1	Cltc	Q5SXR6	1.152	0.991	0.911	1.024
Zinc finger protein 521	Zfp521	Q6KAS7-1	1.027	0.864	0.810	0.785
Protein argonaute-3	Ago3;Eif2c3	Q8CJF9	0.990	1.059	no value	no value

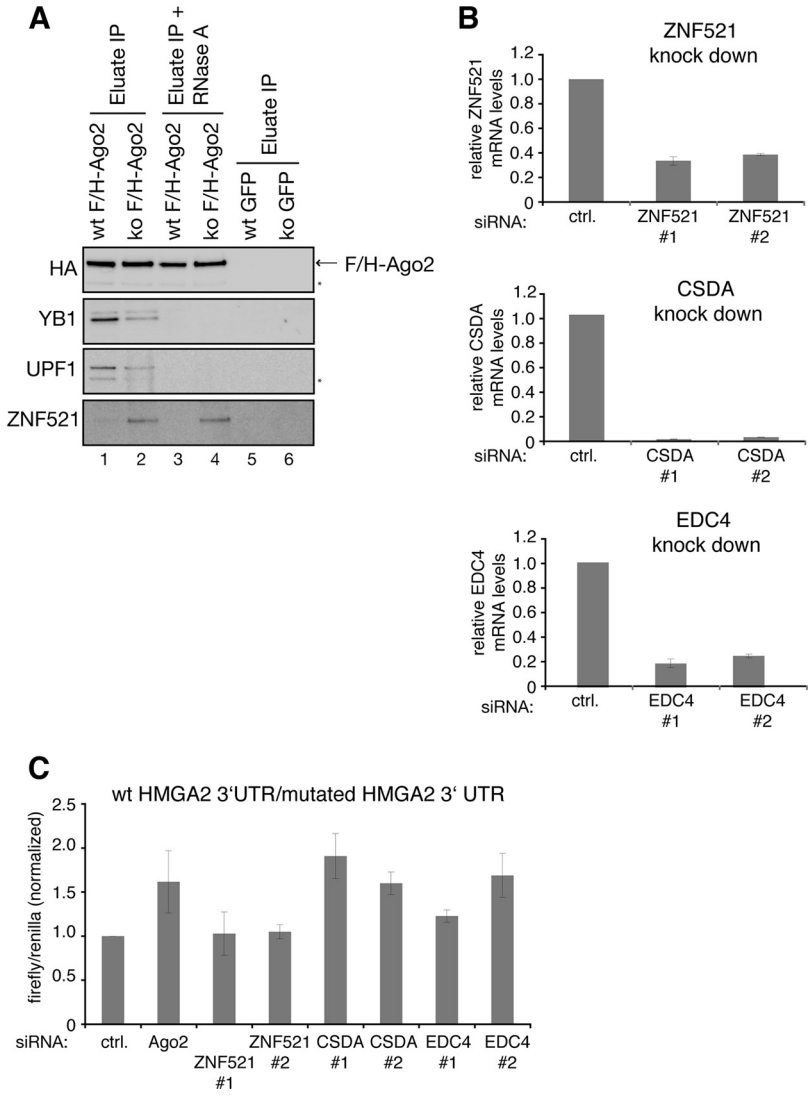

FIG. 4. **Western blot Analysis of identified Ago2 interactors.** *A*, F/H-Ago2 (lanes 1–4) or F/H-GFP (lanes 5 and 6) was immunoprecipitated from the MEFs using anti-FLAG antibodies. To analyze the mRNA dependence of the interaction, the samples were treated with RNase A (lanes 3 and 4). Arrows indicate signals specific for the target protein and asterisks indicate background signals. *B*, Knock down validation by quantitative PCR (qPCR). Total RNA was reverse transcribed and cDNA was amplified using primers specific to ZNF521 (*upper* panel), CSDA (*middle* panel) and EDC4 (*lower* panel). mRNA levels relative to GAPDH mRNA were normalized to control transfections. Values are representative for three different experiments. *C*, Short interfering RNAs against the indicated proteins were pretransfected into HeLa cells. After 2 days, a luciferase reporter containing the 3′ UTR of HMGA2 or a mutated HMGA2 3′-UTR lacking the let-7 binding sites were transfected. Mean Firefly/Renilla ratios from seven independent experiments are displayed. HMGA2 values were normalized to those of the mutated vector.

Validation of Ago2 Interactions—To further verify our mass spectrometry results, we performed Western blot analyses on a set of identified Ago2 interactors (Fig. 4*A*). Ago2 complexes were isolated from FH-Ago2-expressing cells (Fig. 4*A*, lanes 1–4). To test RNA requirements of the interactors, a set of samples was treated with RNase A (Fig. 4*A*, lanes 3 and 4). Immunoprecipitates from the GFP-expressing control cell lines served as background control (Fig. 4*A*, lanes 5 and 6). YBX1 and UPF1 are both miRNA- and mRNA-dependent interactors. We see a strong signal in the Dicer wt sample (Fig. 4*A*, lane 1) and a reduced signal in the Dicer −/− cells (Fig. 4*A*, lane 2) suggesting a miRNA-dependent interaction. This binding is bridged by mRNAs as apparent from the disappearance of the signal after RNase A treatment (lanes 3 and 4). ZNF521 is a protein that directly interacts with Ago2 in the absence of miRNAs and Dicer. As expected, we see signals in the samples from the Dicer −/− cells only (lane 2) and the signal intensity is not affected by the RNase A treatment (lane 4).

To functionally validate our interaction data, we used luciferase-based miRNA reporters (Figs. 4*B* and 4*C*). The 3′ UTR of Hmga2, a well-characterized let-7a target (64), was fused to firefly luciferase and transfected into HeLa cells in which ZNF521, CSDA and EDC4 were depleted by RNAi (Figs. 4*B* and 4*C*). In addition, we employed a reporter containing the Hmga2 3′ UTR with mutated let-7a target sites and normalized the data against each other (19) (Fig. 4*C*). As expected, Ago2 knock down led to increased luciferase activity. Knock down of EDC4, which has been implicated in miRNA function in *Drosophila* (52), resulted in specific luciferase up-regulation as well, suggesting that EDC4 is indeed involved in silencing of the Hmga2 reporter construct. Similar results were obtained for the mRNP component CSDA. ZNF521, however, is not involved in miRNA-guided gene silencing. Since ZNF521 is a putative transcription factor, it is possible that it cooperates with Ago2 in nuclear Ago functions.

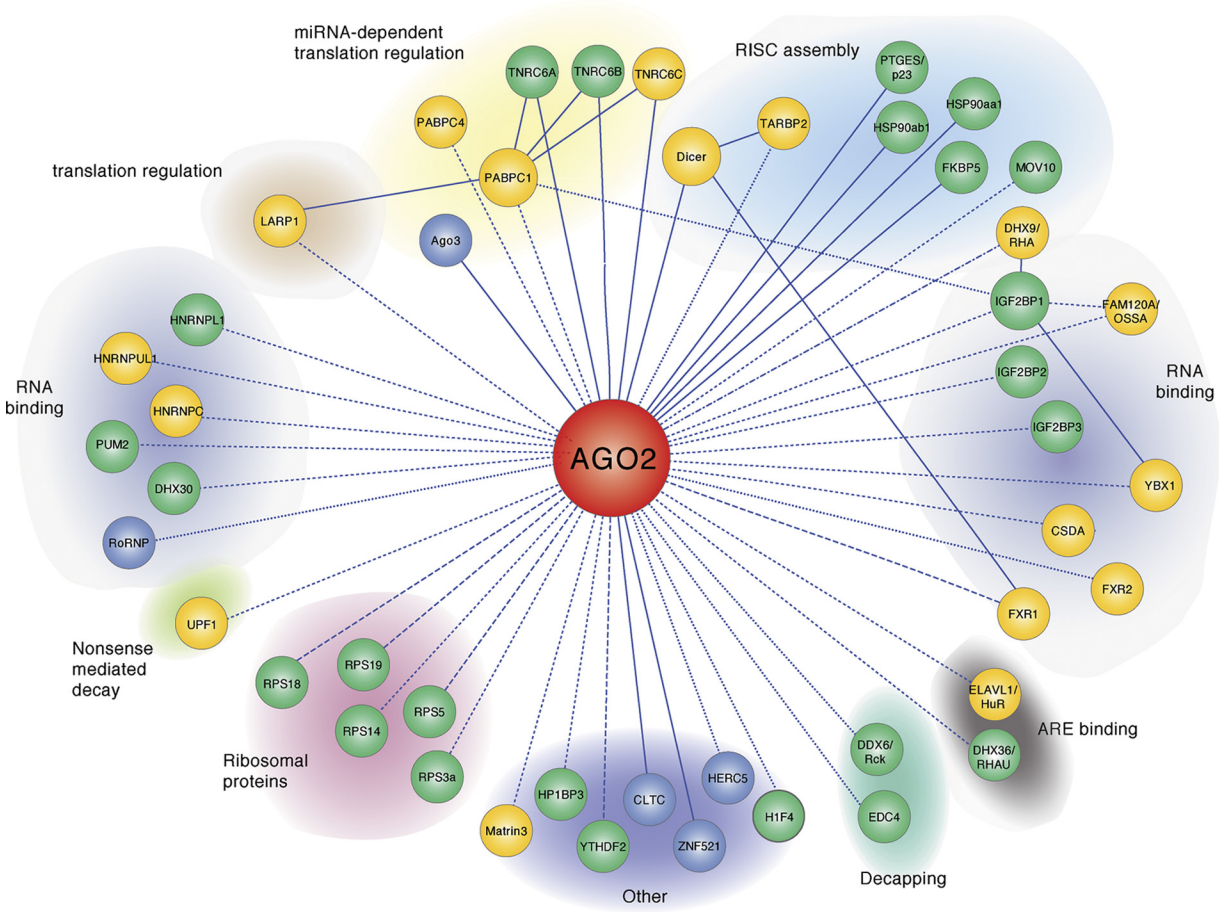

FIG. 5. **Interaction Network of miRNA- and mRNA-dependent Ago2-associated proteins.** The proteomic data was combined into an interaction network. Proteins were grouped according to their biological functions and reported interactions between the Ago2-associated proteins were added. Ago2 is depicted in red. Proteins interacting with Ago2 independently of the miRNA loading status of Ago2 are shown in green. Interactors binding to Ago2 only in the presence or absence of miRNAs are indicated in yellow or blue. The style of the connecting lines represents the mRNA dependence. Solid lines indicate direct protein-protein interactions. Short dashed lines represent a strong mRNA dependence of the interactions. A weak influence of mRNA presence on the binding behavior is depicted by long dashed lines. Broken dashed lines indicate differential mRNA dependences in the presence of absence of miRNAs. Proteins not identified in the mRNA dependence screen are connected to Ago2 by dotted lines.

In summary, our validation experiments show that novel Ago2 interactors discovered by proteomics can play roles in miRNA-guided gene silencing, highlighting the specificity of our Ago2 interaction network.

DISCUSSION

Although several proteomic and genetic studies aiming at the identification of human Ago interaction partners have been performed they have not discriminated between protein-protein or protein-RNA interactions within Ago protein complexes. Using a powerful quantitative proteomic approach based on SILAC and combined with a Dicer-free cell system, we discovered and classified sets of proteins that bind either by protein-protein interaction or indirectly via RNAs to mouse Ago2.

To analyze Ago2 interactions, we used MEFs in which Dicer has been genetically inactivated. As a consequence, miRNA precursors are not processed and therefore mature miRNAs are not produced. It has been shown that miR-451 is processed by Ago2 independently of Dicer (65, 66). miR-451 is not expressed in the MEFs used here (data not shown) and since no other Dicer-independent miRNA has been reported, Ago2 protein complexes are thought to be miRNA free. However, it has been shown recently that many larger non-coding RNA species such as tRNAs or snoRNAs can give rise to small RNAs and the processing of some of these RNAs might even be Dicer-independent (67–70). To rule out that other so far not characterized Dicer-independent small RNAs guide Ago2 to larger RNAs in the absence of Dicer, we analyzed an Ago2 mutant that is not capable of small RNA binding (71). Preliminary experiments revealed that this mutant might still associate with larger RNAs suggesting that Ago2 is recruited to such RNAs without guidance of small RNAs (data not shown).

MiRNAs are viewed as guides that sequence-specifically target Ago protein complexes to distinct sites on mRNAs (3, 10, 72). Very recently, Ago2-mRNA interactions were analyzed in mouse embryonic stem (ES) cells lacking Dicer using RNA-protein cross linking followed by RNA-seq (73). Interestingly, the authors reported that Ago2 indeed interacts with mRNAs in the absence of Dicer. These results together with our SILAC data suggest that Ago2-mRNA interactions can be independent of small RNAs. Two scenarios of how Ago2 contacts larger RNAs independently of small RNAs might be envisioned. First, Ago2 itself might possess RNA-binding activity toward larger RNAs. This is unlikely, because Ago2 binding affinity toward single stranded RNAs peaks at 21 nucleotides and rapidly decreases with the length of the RNA. Second and more likely, a set of RNA binding proteins may be involved in recruiting Ago2 proteins to mRNAs. Consistently, it has been reported recently that a complex composed of Pumillio, Ago proteins and eEF1A regulate translation and this regulation might be independent of miRNA binding (74). Many RNA-binding proteins co-purify with Ago proteins and these proteins may help stabilizing Ago-mRNA interactions (17, 18).

Hypothesizing that unloaded (miRNA-free) Ago complexes interact with different proteins than Ago proteins that are bound to miRNAs, we compared Ago2 complexes from wt and Dicer-deficient MEFs. Indeed, we found a number of proteins that interact with Ago2 specifically in the absence or the presence of Dicer whereas several proteins interact with Ago2 under both conditions. Our data allows for a detailed mapping of the Ago2 interaction network in MEFs (Fig. 5). Proteins that interact independently of Dicer are shown in green, proteins that require Dicer for the interaction with Ago2 in yellow and proteins that only interact in the absence of Dicer are shown in blue. Strikingly, our proteomics experiments recapitulate all factors that have been implicated in RISC loading or miRNA function so far. In addition we find a number of RNA binding proteins, translational regulators, five ribosomal proteins as well as decapping activators. There are only six other proteins (gray). We note that our approach could be used to analyze whether or not the Ago1, Ago3 and Ago4 interaction networks are identical with the Ago2 network or whether there are differences.

The current model of the mechanism of miRNA-guided gene silencing is that Ago proteins interact with a member of the GW128 protein family, which in turn interacts with a protein binding to the poly(A) tail of the mRNA. This leads to an inhibition of the interaction of PABP with the cap binding complex resulting in reduced translational initiation. GW182 recruits the CCR4/NOT complex to the poly(A) tail, which removes the poly(A) tail leading to decapping and mRNA degradation from the 5′ end. Our proteomics data reveals several interesting interactions with regards to the mechanism of miRNA function.

First, although the interactions of the miRNA machinery with deadenylase complexes has been characterized in molecular detail (75–77), not much is known about possible functional interactions of the Ago-miRNA complex with the decapping machinery. Based on our observation that EDC4 interacts with Ago2, it is tempting to speculate that Ago proteins not only stimulate deadenylation via the GW182 proteins but also subsequent decapping via EDC4 leading to efficient mRNA decay and gene silencing. In support of such a model, it has been found that fly EDC4 protein (also referred to as Ge-1) is required for miRNA-guided gene silencing in *Drosophila* cells (52).

Second, the three mammalian GW-protein TNRC6A, B and C have been implicated in miRNA-guided gene silencing. However, individual functional differences have not been reported. Here, we find that TNRC6A and B interact with Ago2 both in the absence and presence of miRNAs. However, TNRC6C is only found together with Ago2 when miRNAs are processed. We speculate that TNRC6C may only interact with Ago2 on specific mRNA targets while TNRC6A and B interact with Ago2 also in the absence of target RNAs. Alternatively, TNRC6C could be directly recruited to Ago2 by Dicer. Our proteomic data serve to elucidate this and related questions in targeted functional experiments.

Acknowledgments—We thank Daniela Vogg for technical assistance and Anne Dueck for help with Northern blotting.

* This work was in part supported by the Max-Planck Society for the Advancement of Science and by grants from the Deutsche Forschungsgemeinschaft (SFB 960 to G.M.), the European Research Council (ERC grant 'sRNAs' to G.M.) and the Bavarian Genome Research Network (BayGene to G.M.).

S This article contains supplemental Fig. S1 and Tables S1 and S2.

** To whom correspondence should be addressed: Laboratory of RNA Biology, University of Regensburg, Universitätsstraße 31, 93053 Regensburg, Deutschland/Germany. Tel.: +49 941 943 2847; Fax: +49 941 943 2936; E-mail: gunter.meister@vkl.uni-regensburg.de.

‡‡ Present address: Genentech, Inc., 1 DNA Way, South San Francisco, CA 94080, USA.

REFERENCES

1. Ender, C., and Meister, G. (2010) Argonaute proteins at a glance. *J. Cell Sci.* **123,** 1819–1823
2. Hutvagner, G., and Simard, M. J. (2008) Argonaute proteins: key players in RNA silencing. *Nat. Rev. Mol. Cell Biol.* **9,** 22–32
3. Meister, G., and Tuschl, T. (2004) Mechanisms of gene silencing by double-stranded RNA. *Nature* **431,** 343–349
4. Carthew, R. W., and Sontheimer, E. J. (2009) Origins and Mechanisms of miRNAs and siRNAs. *Cell* **136,** 642–655
5. Siomi, H., and Siomi, M. C. (2009) On the road to reading the RNA-interference code. *Nature* **457,** 396–404
6. Jinek, M., and Doudna, J. A. (2009) A three-dimensional view of the molecular machinery of RNA interference. *Nature* **457,** 405–412
7. Meister, G., Landthaler, M., Patkaniowska, A., Dorsett, Y., Teng, G., and Tuschl, T. (2004) Human Argonaute2 Mediates RNA Cleavage Targeted by miRNAs and siRNAs. *Mol. Cell* **15,** 185–197
8. Liu, J., Carmell, M. A., Rivas, F. V., Marsden, C. G., Thomson, J. M., Song, J. J., Hammond, S. M., Joshua-Tor, L., and Hannon, G. J. (2004) Argonaute2 is the catalytic engine of mammalian RNAi. *Science* **305,** 1437–1441
9. Kim, V. N., Han, J., and Siomi, M. C. (2009) Biogenesis of small RNAs in animals. *Nat. Rev. Mol. Cell Biol.* **10,** 126–139

10. Bartel, D. P. (2009) MicroRNAs: target recognition and regulatory functions. *Cell* **136,** 215–233
11. Krol, J., Loedige, I., and Filipowicz, W. (2010) The widespread regulation of microRNA biogenesis, function and decay. *Nat. Rev. Genet.* **11,** 597–610
12. Huntzinger, E., and Izaurralde, E. (2011) Gene silencing by microRNAs: contributions of translational repression and mRNA decay. *Nat. Rev. Genet.* **12,** 99–110
13. Winter, J., Jung, S., Keller, S., Gregory, R. I., and Diederichs, S. (2009) Many roads to maturity: microRNA biogenesis pathways and their regulation. *Nat. Cell Biol.* **11,** 228–234
14. Qi, H. H., Ongusaha, P. P., Myllyharju, J., Cheng, D., Pakkanen, O., Shi, Y., Lee, S. W., Peng, J. and Shi, Y. (2008) Prolyl 4-hydroxylation regulates Argonaute 2 stability. *Nature* **455,** 421–424
15. Rybak, A., Fuchs, H., Hadian, K., Smirnova, L., Wulczyn, E. A., Michel, G., Nitsch, R., Krappmann, D., and Wulczyn, F. G. (2009) The let-7 target gene mouse lin-41 is a stem cell specific E3 ubiquitin ligase for the miRNA pathway protein Ago2. *Nat. Cell Biol.* **11,** 1411–1420
16. Rüdel, S., Wang, Y., Lenobel, R., Körner, R., Hsiao, H. H., Urlaub, H., Patel, D., and Meister, G. (2011) Phosphorylation of human Argonaute proteins affects small RNA binding. *Nucleic Acids Res.* **39,** 2330–2343
17. Höck, J., Weinmann, L., Ender, C., Rüdel, S., Kremmer, E., Raabe, M., Urlaub, H., and Meister, G. (2007) Proteomic and functional analysis of Argonaute-containing mRNA-protein complexes in human cells. *EMBO Rep.* **8,** 1052–1060
18. Landthaler, M., Gaidatzis, D., Rothballer, A., Chen, P. Y., Soll, S. J., Dinic, L., Ojo, T., Hafner, M., Zavolan, M., and Tuschl, T. (2008) Molecular characterization of human Argonaute-containing ribonucleoprotein complexes and their bound target mRNAs. *RNA* **14,** 2580–2596
19. Weinmann, L., Höck, J., Ivacevic, T., Ohrt, T., Mütze, J., Schwille, P., Kremmer, E., Benes, V., Urlaub, H., and Meister, G. (2009) Importin 8 is a gene silencing factor that targets argonaute proteins to distinct mRNAs. *Cell* **136,** 496–507
20. Kedde, M., Strasser, M. J., Boldajipour, B., Vrielink, J. A., Slanchev, K., le Sage, C., Nagel, R., Voorhoeve, P. M., van Duijse, J., Ørom, U. A., Lund, A. H., Perrakis, A., Raz, E., and Agami, R. (2007) RNA-binding protein Dnd1 inhibits microRNA access to target mRNA. *Cell* **131,** 1273–1286
21. Bhattacharyya, S. N., Habermacher, R., Martine, U., Closs, E. I., and Filipowicz, W. (2006) Relief of microRNA-mediated translational repression in human cells subjected to stress. *Cell* **125,** 1111–1124
22. Eiring, A. M., Harb, J. G., Neviani, P., Garton, C., Oaks, J. J., Spizzo, R., Liu, S., Schwind, S., Santhanam, R., Hickey, C. J., Becker, H., Chandler, J. C., Andino, R., Cortes, J., Hokland, P., Huettner, C. S., Bhatia, R., Roy, D. C., Liebhaber, S. A., Caligiuri, M. A., Marcucci, G., Garzon, R., Croce, C. M., Calin, G. A., and Perrotti, D. (2010) miR-328 functions as an RNA decoy to modulate hnRNP E2 regulation of mRNA translation in leukemic blasts. *Cell* **140,** 652–665
23. Gingras, A. C., Gstaiger, M., Raught, B., and Aebersold, R. (2007) Analysis of protein complexes using mass spectrometry. *Nat. Rev. Mol. Cell Biol.* **8,** 645–654
24. Blagoev, B., Kratchmarova, I., Ong, S. E., Nielsen, M., Foster, L. J., and Mann, M. (2003) A proteomics strategy to elucidate functional protein-protein interactions applied to EGF signaling. *Nat. Biotechnol*. **21,** 315–318
25. Ranish, J. A., Yi, E. C., Leslie, D. M., Purvine, S. O., Goodlett, D. R., Eng, J., and Aebersold, R. (2003) The study of macromolecular complexes by quantitative proteomics. *Nat. Genet.* **33,** 349–355
26. Vermeulen, M., Hubner, N. C., and Mann, M. (2008) High confidence determination of specific protein-protein interactions using quantitative mass spectrometry. *Curr. Opin. Biotechnol*. **19,** 331–337
27. Mann, M. (2006) Functional and quantitative proteomics using SILAC. *Nat. Rev. Mol. Cell Biol.* **7,** 952–958
28. Hilger, M., and Mann, M. (2011) Triple SILAC to Determine Stimulus Specific Interactions in the Wnt Pathway. *J. Proteome Res.* **11,** 982–994
29. Trinkle-Mulcahy, L., Andersen, J., Lam, Y. W., Moorhead, G., Mann, M., and Lamond, A. I. (2006) Repo-Man recruits PP1 gamma to chromatin and is essential for cell viability. *J. Cell Biol.* **172,** 679–692
30. Schwanhäusser, B., Gossen, M., Dittmar, G., and Selbach, M. (2009) Global analysis of cellular protein translation by pulsed SILAC. *Proteomics* **9,** 205–209
31. Vinther, J., Hedegaard, M. M., Gardner, P. P., Andersen, J. S., and Arctander, P. (2006) Identification of miRNA targets with stable isotope labeling by amino acids in cell culture. *Nucleic Acids Res.* **34,** e107
32. Selbach, M., Schwanhäusser, B., Thierfelder, N., Fang, Z., Khanin, R., and Rajewsky, N. (2008) Widespread changes in protein synthesis induced by microRNAs. *Nature* **455,** 58–63
33. Baek, D., Villén, J., Shin, C., Camargo, F. D., Gygi, S. P., and Bartel, D. P. (2008) The impact of microRNAs on protein output. *Nature* **455,** 64–71
34. Meister, G., Landthaler, M., Peters, L., Chen, P. Y., Urlaub, H., Lührmann, R., and Tuschl, T. (2005) Identification of novel argonaute-associated proteins. *Curr. Biol.* **15,** 2149–2155
35. Murchison, E. P., Partridge, J. F., Tam, O. H., Cheloufi, S., and Hannon, G. J. (2005) Characterization of Dicer-deficient murine embryonic stem cells. *Proc. Natl. Acad. Sci. U.S.A.* **102,** 12135–12140
36. Kanellopoulou, C., Muljo, S. A., Kung, A. L., Ganesan, S., Drapkin, R., Jenuwein, T., Livingston, D. M., and Rajewsky, K. (2005) Dicer-deficient mouse embryonic stem cells are defective in differentiation and centromeric silencing. *Genes Dev.* **19,** 489–501
37. Glasmacher, E., Hoefig, K. P., Vogel, K. U., Rath, N., Du, L., Wolf, C., Kremmer, E., Wang, X., and Heissmeyer, V. (2010) Roquin binds inducible costimulator mRNA and effectors of mRNA decay to induce microRNA-independent post-transcriptional repression. *Nat. Immunol.* **11,** 725–733
38. Calabrese, J. M., Seila, A. C., Yeo, G. W., and Sharp, P. A. (2007) RNA sequence analysis defines Dicer's role in mouse embryonic stem cells. *Proc. Natl. Acad. Sci. U.S.A.* **104,** 18097–18102
39. Leung, A. K., Calabrese, J. M., and Sharp, P. A. (2006) Quantitative analysis of Argonaute protein reveals microRNA-dependent localization to stress granules. *Proc. Natl. Acad. Sci. U.S.A.* **103,** 18125–18130
40. Shevchenko, A., Tomas, H., Havlis, J., Olsen, J. V., and Mann, M. (2006) In-gel digestion for mass spectrometric characterization of proteins and proteomes. *Nat. Protoc.* **1,** 2856–2860
41. Rappsilber, J., Ishihama, Y., and Mann, M. (2003) Stop and go extraction tips for matrix-assisted laser desorption/ionization, nanoelectrospray, and LC/MS sample pretreatment in proteomics. *Anal. Chem.* **75,** 663–670
42. Rappsilber, J., Mann, M., and Ishihama, Y. (2007) Protocol for micro-purification, enrichment, pre-fractionation and storage of peptides for proteomics using StageTips. *Nat. Protoc.* **2,** 1896–1906
43. Olsen, J. V., de Godoy, L. M., Li, G., Macek, B., Mortensen, P., Pesch, R., Makarov, A., Lange, O., Horning, S., and Mann, M. (2005) Parts per million mass accuracy on an Orbitrap mass spectrometer via lock mass injection into a C-trap. *Mol. Cell Proteomics* **4,** 2010–2021
44. Cox, J., and Mann, M. (2008) MaxQuant enables high peptide identification rates, individualized p.p.b.-range mass accuracies and proteome-wide protein quantification. *Nat. Biotechnol*. **26,** 1367–1372
45. Cox, J., Neuhauser, N., Michalski, A., Scheltema, R. A., Olsen, J. V., and Mann, M. (2011) Andromeda: a peptide search engine integrated into the MaxQuant environment. *J. Proteome Res*. **10,** 1794–1805
46. Wang, X., and Huang, L. (2008) Identifying dynamic interactors of protein complexes by quantitative mass spectrometry. *Mol. Cell. Proteomics* **7,** 46–57
47. Mousson, F., Kolkman, A., Pijnappel, W. W., Timmers, H. T., and Heck, A. J. (2008) Quantitative proteomics reveals regulation of dynamic components within TATA-binding protein (TBP) transcription complexes. *Mol. Cell. Proteomics* **7,** 845–852
48. Iki, T., Yoshikawa, M., Nishikiori, M., Jaudal, M. C., Matsumoto-Yokoyama, E., Mitsuhara, I., Meshi, T., and Ishikawa, M. (2010) In vitro assembly of plant RNA-induced silencing complexes facilitated by molecular chaperone HSP90. *Mol. Cell* **39,** 282–291
49. Iwasaki, S., Kobayashi, M., Yoda, M., Sakaguchi, Y., Katsuma, S., Suzuki, T., and Tomari, Y. (2010) Hsc70/Hsp90 chaperone machinery mediates ATP-dependent RISC loading of small RNA duplexes. *Mol. Cell* **39,** 292–299
50. Pare, J. M., Tahbaz, N., Lopez-Orozco, J., LaPointe, P., Lasko, P., and Hobman, T. C. (2009) Hsp90 regulates the function of argonaute 2 and its recruitment to stress granules and P-bodies. *Mol. Biol. Cell* **20,** 3273–3284
51. Jin, H., Suh, M. R., Han, J., Yeom, K. H., Lee, Y., Heo, I., Ha, M., Hyun, S., and Kim, V. N. (2009) Human UPF1 participates in small RNA-induced mRNA downregulation. *Mol. Cell Biol.* **29,** 5789–5799
52. Eulalio, A., Rehwinkel, J., Stricker, M., Huntzinger, E., Yang, S. F., Doerks, T., Dorner, S., Bork, P., Boutros, M., and Izaurralde, E. (2007) Target-

specific requirements for enhancers of decapping in miRNA-mediated gene silencing. *Genes Dev.* **21,** 2558–2570
53. Chu, C. Y., and Rana, T. M. (2006) Translation repression in human cells by microRNA-induced gene silencing requires RCK/p54. *PLoS Biol*. **4,** e210
54. Grimmler, M., Otter, S., Peter, C., Müller, F., Chari, A., and Fischer, U. (2005) Unrip, a factor implicated in cap-independent translation, associates with the cytosolic SMN complex and influences its intracellular localization. *Hum. Mol. Genet.* **14,** 3099–3111
55. Duncan, K. E., Strein, C., and Hentze, M. W. (2009) The SXL-UNR corepressor complex uses a PABP-mediated mechanism to inhibit ribosome recruitment to msl-2 mRNA. *Mol. Cell* **36,** 571–582
56. Chendrimada, T. P., Gregory, R. I., Kumaraswamy, E., Norman, J., Cooch, N., Nishikura, K., and Shiekhattar, R. (2005) TRBP recruits the Dicer complex to Ago2 for microRNA processing and gene silencing. *Nature* **436,** 740–744
57. Haase, A. D., Jaskiewicz, L., Zhang, H., Lainé, S., Sack, R., Gatignol, A., and Filipowicz, W. (2005) TRBP, a regulator of cellular PKR and HIV-1 virus expression, interacts with Dicer and functions in RNA silencing. *EMBO Rep*. **6,** 961–967
58. Robb, G. B., and Rana, T. M. (2007) RNA Helicase A Interacts with RISC in Human Cells and Functions in RISC Loading. *Mol. Cell* **26,** 523–537
59. Burrows, C., Abd Latip, N., Lam, S. J., Carpenter, L., Sawicka, K., Tzolovsky, G., Gabra, H., Bushell, M., Glover, D. M., Willis, A. E., and Blagden, S. P. (2010) The RNA binding protein Larp1 regulates cell division, apoptosis and cell migration. *Nucleic Acids Res.* **38,** 5542–5553
60. Belisova, A., Semrad, K., Mayer, O., Kocian, G., Waigmann, E., Schroeder, R., and Steiner, G. (2005) RNA chaperone activity of protein components of human Ro RNPs. *RNA* **11,** 1084–1094
61. Bond, H. M., Mesuraca, M., Amodio, N., Mega, T., Agosti, V., Fanello, D., Pelaggi, D., Bullinger, L., Grieco, M., Moore, M. A., Venuta, S., and Morrone, G. (2008) Early hematopoietic zinc finger protein-zinc finger protein 521: a candidate regulator of diverse immature cells. *Int. J. Biochem. Cell Biol.* **40,** 848–854
62. Wong, J. J., Pung, Y. F., Sze, N. S., and Chin, K. C. (2006) HERC5 is an IFN-induced HECT-type E3 protein ligase that mediates type I IFN-induced ISGylation of protein targets. *Proc. Natl. Acad. Sci. U.S.A.* **103,** 10735–10740
63. Chan, S. P., and Slack, F. J. (2009) Ribosomal protein RPS-14 modulates let-7 microRNA function in Caenorhabditis elegans. *Dev. Biol.* **334,** 152–160
64. Mayr, C., Hemann, M. T., and Bartel, D. P. (2007) Disrupting the pairing between let-7 and Hmga2 enhances oncogenic transformation. *Science* **315,** 1576–1579
65. Cheloufi, S., Dos Santos, C. O., Chong, M. M., and Hannon, G. J. (2010) A dicer-independent miRNA biogenesis pathway that requires Ago catalysis. *Nature* **465,** 584–589
66. Cifuentes, D., Xue, H., Taylor, D. W., Patnode, H., Mishima, Y., Cheloufi, S., Ma, E., Mane, S., Hannon, G. J., Lawson, N. D., Wolfe, S. A., and Giraldez, A. J. (2010) A novel miRNA processing pathway independent of Dicer requires Argonaute2 catalytic activity. *Science* **328,** 1694–1698
67. Taft, R. J., Glazov, E. A., Lassmann, T., Hayashizaki, Y., Carninci, P., and Mattick, J. S. (2009) Small RNAs derived from snoRNAs. *RNA* **15,** 1233–1240
68. Ender, C., Krek, A., Friedlander, M. R., Beitzinger, M., Weinmann, L., Chen, W., Pfeffer, S., Rajewsky, N., and Meister, G. (2008) A Human snoRNA with MicroRNA-Like Functions. *Mol. Cell* **32,** 519–528
69. Haussecker, D., Huang, Y., Lau, A., Parameswaran, P., Fire, A. Z., and Kay, M. A. (2010) Human tRNA-derived small RNAs in the global regulation of RNA silencing. *RNA* **16,** 673–695
70. Scott, M. S., and Ono, M. (2011) From snoRNA to miRNA: Dual function regulatory non-coding RNAs. *Biochimie* **93,** 1987–1992
71. Rüdel, S., Flatley, A., Weinmann, L., Kremmer, E., and Meister, G. (2008) A multifunctional human Argonaute2-specific monoclonal antibody. *RNA* **14,** 1244–1253
72. Schwarz, D. S., Hutvágner, G., Haley, B., and Zamore, P. D. (2002) Evidence that siRNAs function as guides, not primers, in the Drosophila and human RNAi pathways. *Mol. Cell* **10,** 537–548
73. Leung, A. K., Young, A. G., Bhutkar, A., Zheng, G. X., Bosson, A. D., Nielsen, C. B., and Sharp, P. A. (2011) Genome-wide identification of Ago2 binding sites from mouse embryonic stem cells with and without mature microRNAs. *Nat. Struct. Mol. Biol*. **18,** 237–244
74. Friend, K., Campbell, Z. T., Cooke, A., Kroll-Conner, P., Wickens, M. P., and Kimble, J. (2012) A conserved PUF-Ago-eEF1A complex attenuates translation elongation. *Nat. Struct. Mol. Biol.* **19,** 176–183
75. Braun, J. E., Huntzinger, E., Fauser, M., and Izaurralde, E. (2011) GW182 proteins directly recruit cytoplasmic deadenylase complexes to miRNA targets. *Mol. Cell* **44,** 120–133
76. Chekulaeva, M., Mathys, H., Zipprich, J. T., Attig, J., Colic, M., Parker, R., and Filipowicz, W. (2011) miRNA repression involves GW182-mediated recruitment of CCR4-NOT through conserved W-containing motifs. *Nat. Struct. Mol. Biol*. **18,** 1218–1226
77. Fabian, M. R., Cieplak, M. K., Frank, F., Morita, M., Green, J., Srikumar, T., Nagar, B., Yamamoto, T., Raught, B., Duchaine, T. F., and Sonenberg, N. (2011) miRNA-mediated deadenylation is orchestrated by GW182 through two conserved motifs that interact with CCR4-NOT. *Nat. Struct. Mol. Biol*. **18,** 1211–1217